Cement & Concrete Composites 30 (2008) 679–685

Contents lists available at ScienceDirect

Cement & Concrete Composites

journal homepage: www.elsevier.com/locate/cemconcomp

Mechanical activation of granulated blast furnace slag and its effect on the properties and structure of portland slag cement

Sanjay Kumar *, Rakesh Kumar, A. Bandopadhyay, T.C. Alex, B. Ravi Kumar, S.K. Das, S.P. Mehrotra

National Metallurgical Laboratory (CSIR), Jamshedpur 831 007, India

ARTICLE INFO

Article history:
Received 15 February 2006
Received in revised form 12 May 2008
Accepted 13 May 2008
Available online 28 May 2008

Keywords:
Mechanical activation
Granulated blast furnace slag
Microstructure
Compressive strength
Blended cement

ABSTRACT

Mechanically activated granulated blast furnace slag (GBFS) was used in the range of 50–95% to replace clinker in portland slag cement (PSC). The slag and clinker were activated separately using an attrition mill and mixed to prepare cement formulations. Use of activated slag resulted in a remarkable increase in strength vis-à-vis commercial slag cement. Both 1-day and 28-day strength were found to increase with an increase in slag content up to 70%. The strength of the sample containing 80–85% slag was comparable to the commercial cement used as a reference. It was observed that mechanical activation of slag was more critical from the point of view of strength development. The hydrated cement samples were characterised using powder X-ray diffraction (XRD), scanning electron microscopy with X-ray microanalysis (SEM-EDS) and simultaneous thermogravimetry and differential thermal analysis (TG/DTA). It is established that microstructural changes resulting from enhanced reactivity of slag and densification are related with the improvement in cement strength.

© 2008 Elsevier Ltd. All rights reserved.

1. Introduction

Granulated blast furnace slag (GBFS) is the by-product of iron making process and is produced by water quenching of molten blast furnace slag. For its use in blended cements, GBFS is ground to improve its reactivity during cement hydration. The main constituents of GBFS include CaO, SiO_2, and Al_2O_3. In addition, it contains small amount of MgO, FeO, and sulphide as CaS, MnS, and FeS. Slag shows primarily cementitious behaviour (latent hydraulic activity) but may show some pozzolanic character (reaction with lime) as well. The activity of GBFS is determined by the quantities and the properties of amorphous glass, as well as the chemical compositions.

Use of GBFS as cement replacement in concrete is a common practice due to technological, economic, and environmental benefits. Enhancement in mechanical properties and resistance to scaling and chloride ion penetration was reported when GBFS used in binary and ternary blended cement concretes and hydrated for 28 days or more [1,2]. Worldwide, the use of large volume of slag in blended cements has attracted significant research attention [3–5]. The replacement of cement clinker by GBFS usually results in lower early strength and longer setting times, and restricts the use of large proportion of slag in portland slag cement (PSC). Fine grinding and mechanical activation [6,7] was suggested to improve the reactivity of the blended cement constituents [8–10]. Fine grinding leads to generation of larger surface area, whereas mechanical activation results from combined effect of particle breakage (surface area) and other bulk and surface physicochemical changes, dislocations and other defects induced by the milling [3,4,7]. Due to enhanced reactivity, the resulting cement and/or concrete exhibits improved strength and setting properties [8–11]. Various types of milling devices were tried for the mechanical activation of cement constituents [8–13]. The merit of attrition mills for the mechanical activation of cement constituents was recognized [9,10]. Attrition mills, also known as stirred ball mills, agitator beads mills or agitator mills have emerged as efficient milling devices for fine grinding and production of narrow size distribution in the milled products [14–19]. In contrast to conventional ball mills, these mills are equipped with a stationary shell and a high-speed rotor for stirring the grinding media, which, in turn, are significantly smaller in size than the conventional ball mill but occupy a larger volume fraction [16]. High efficiency of these mills result due to smaller size grinding media (2 to <0.5 mm) and high agitator speed (may go up to few thousand rpm). While smaller size of media provides larger contact surface between the media and material being ground (high stress number), higher agitator speed gives rise to greater kinetic energy of the media (stress intensity) [15,18].

Recently, we made a striking observation that complete hydration of the slag is possible without a chemical activator if the slag is mechanically activated in an attrition mill [20]. The slag that was attrition milled in our laboratory for about 30 min or more was found to hydrate completely after 28 days,

* Corresponding author. Tel.: +91 657 2271709 14x2207; fax: +91 657 2270527.
E-mail address: sanjay_kumar_nml@yahoo.com (S. Kumar).

0958-9465/$ - see front matter © 2008 Elsevier Ltd. All rights reserved.
doi:10.1016/j.cemconcomp.2008.05.005

without any chemical or clinker addition. Based on these observations, we have carried out studies on the use of high volume attrition milled slag in blended cements. In the present work, attrition milled slag were used up to 95% to replace clinker in portland slag cement. The results are compared with industrial cement prepared with the same basic raw materials (clinker, slag and gypsum) as used in the present study. The hydrated cement samples are characterized to elucidate the effect of mechanical activation on the hydration process and evolution of microstructure.

2. Materials and methods

Granulated blast furnace slag sample from one of the integrated steel plants in the state of Chattisgarh (India) was used. The chemical composition of the slag (in wt.%) was as follows: SiO_2 – 33.1, Al_2O_3 – 21.6, Fe_2O_3 – 0.87, CaO –33.0, MgO – 8.85. Basicity of slag, defined as $[(CaO + MgO + Al_2O_3)/SiO_2]$ and $[(CaO + MgO + 1/3Al_2O_3)/SiO_2 + 2/3Al_2O_3)]$, was 1.9 and 1, respectively. The glass content of the slag was 93%. Powder X-ray diffraction studies showed that the only crystalline phase present in the slag was gehlenite (C_2AS) [21]. The crystallisation temperature of the slag was 915 °C. The slag was characterised by a median particle size (X_{50}) of 89.8 μm and, its density was 2.88 g/cm^3.

The cement clinker from one of the cement plants in the state of Chattisgarh (India) was used. The chemical composition of the cement (in wt.%) was as follows: SiO_2 – 21.34, Al_2O_3 – 5.92, Fe_2O_3 – 2.89, CaO – 62.75, MgO – 2.16. Quantitative X-ray powder diffraction phase analysis based on Rietveld method [22] using SIROQUANT^{TM} software developed by CSIRO, Australia indicated following mineralogical composition of the clinker: C_3S – 60.6%, C_2S – 21.9%, C_3A – 11.1% and C_4AF – 6.4% (C = CaO, S = SiO_2, A = Al_2O_3, F = Fe_2O_3).

The commercial portland slag cement (labelled as IC-A in subsequent description) containing 40% slag, 55% clinker and 5% gypsum was used as a reference sample. The slag and clinker in this cement was the same used for the study.

Attrition milling was carried out using NETZSCH (Germany) attrition mill (Model: PE-075). Milling of slag was done for 3, 5, 10, 15, 30, 45 and 60 min at 1000 rpm using 2 mm diameter steel balls. SHIMADZU centrifugal particle size analyser was used to determine the particle size distribution. The milled slag samples were also characterised in terms of Zeta potential using Laser Zee meter (Modal 501, Pen Kem, USA). Based on exploratory studies, the GBFS after 10-min attrition milling was used for blended cement formulation and testing. GBFS and clinker were attrition milled separately for 10 minutes and then mixed. 5% gypsum was added in all the cases. The cement samples were prepared with increasing amount of slag and labeled as AMCXS (where AMC means attrition milled clinker, and XS indicate % of attrition milled slag). Sample containing ball milled clinker and 50% attrition milled slag (sample label BMC50S) were also prepared to study the effect of clinker fineness.

The compressive strength was tested on $25 \times 25 \times 25$ mm cubes after 1, 3, 7 and 28 days. The 'cement to aggregate ratio' and 'water to cement ratio', 3 and 0.5, respectively, was maintained constant for all the samples. The hydration of the samples was stopped by repeated washing and immersing in isopropyl alcohol for 1 h and air drying. The hydration of cement phases was studies using powder X-ray diffraction (XRD) technique. XRD patterns were recorded on a Siemens D500 Diffractometer. Microstructural characterisation of the samples was done using scanning electron microscope (JEOL 840 SEM with Kevex EDS detector). The samples were also subjected to thermal analysis by SEIKO simultaneous TG/DTA (Model No. 320, Sensitivity = 1 μg).

3. Results and discussion

3.1. Mechanical activation of slag in attrition mill

The milled slag samples were characterized by isolated angular slag particles. The variation in median size (X_{50}) and Zeta potential of the slag milled for different time up to 60 min is given in Fig. 1. A sharp decrease in the median size (X_{50}) from 85.3 to 14.2 μm is observed during initial stage of milling up to about 5 min. The sharp decrease in size is followed by a moderate decrease in size, typically the value of X_{50} was found to be 9.1 after 15 min. The decrease in size after about 15 min is very slow (X_{50} = 3.9 μm after 60 min milling). The milling of slag not only results in particle breakage but possibility exists for the bulk and surface activation of the slag. The technique employed for structural Characterization, i.e. XRD, did not detect any change in the bulk structure. Characteristic variation in the Zeta potential was observed indicating possibility of surface activation/alteration during the milling. Lowest value of Zeta potential –29 to –30 mV was observed for the samples milled from about 5–15 min. Based on this observation, a 10 min milled slag was used for blended cement formulations.

3.2. Cement formulations based on mechanically activated slag and clinker

Fig. 2 shows the variation in compressive strength with hydration time for the blended slag cement samples AMCXS (XS = 50, 60,. . .,95), commercial cement sample IC-A (40% slag) and pure clinker (without any gypsum). Unlike the earlier studies, where cement containing ball milled slag typically shows strength reduction at early ages (7–20 days), early strength (3 and 7 days) increased in AMCXS samples containing 50–70% mechanically activated slag [23]. A significant increase in the 1 day strength was observed due to mechanical activation. Similar observation was reported when 45% blast furnace slag was used in the mechanically modified cement [24]. The improvement in the strength became less pronounced with an increase in replacement level. The 1 day strength was higher than the commercial sample for all replacement levels up to 95%. Similarly, the 3 and 7 days strength was also higher for AMCXS samples than IC-A except for the sample containing 95% slag (i.e. AMC95S). It is interesting to note that the 28 day strength increased with an increase in slag content up to 70% slag. The 28 day strength of AMC70S was ~2 times higher than

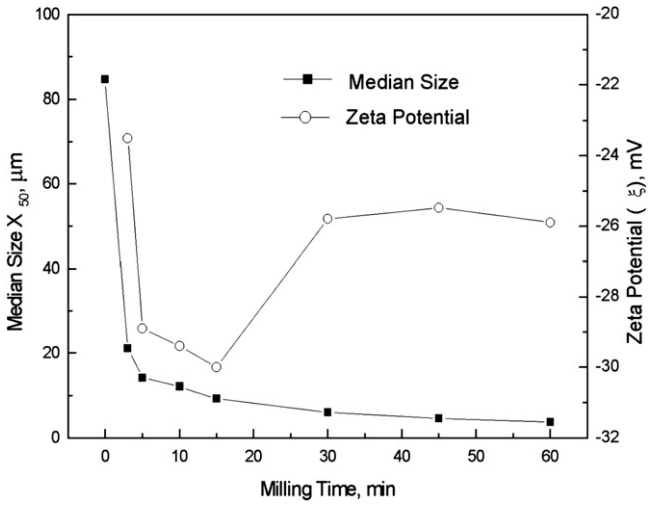

Fig. 1. Variation in median size (X_{50}) and Zeta potential of the slag after different milling time.

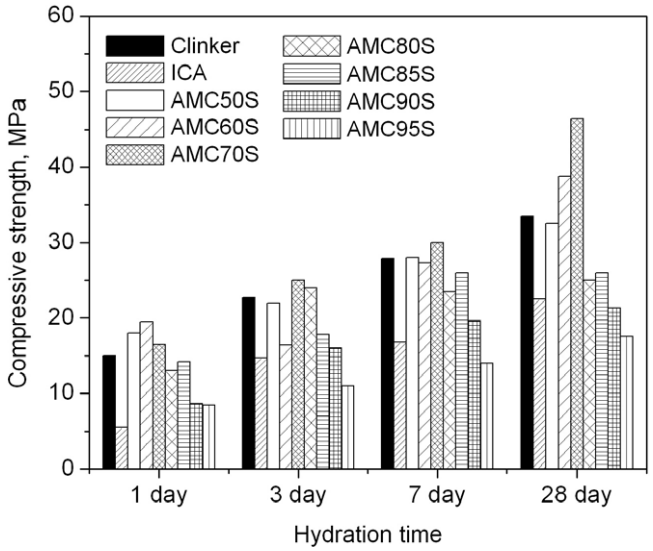

Fig. 2. Variation in compressive strength with hydration time for the AMCXS samples (X = 50–95% activated slag) and IC-A (40% slag).

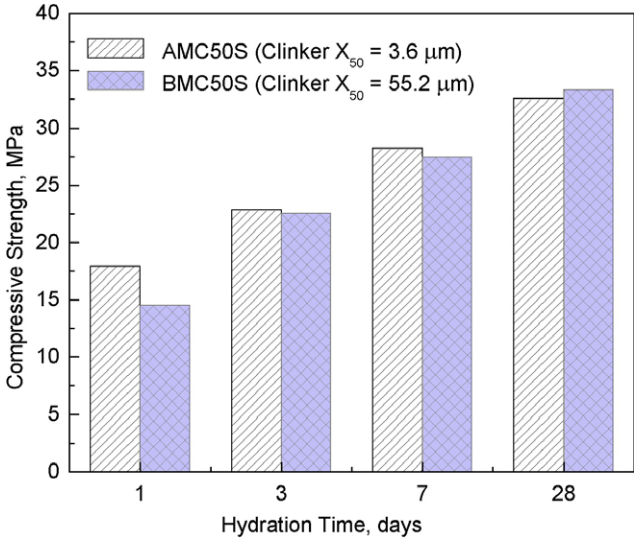

Fig. 3. Variation in compressive strength of cement with time for AMC50S and BMC50S.

the commercial cement (IC-A). The 28 day strength begins to decrease with an increase in slag content beyond 70%. The 28-day strength for AMC80S and AMC85S is higher than IC-A. However, AMC95S showed a lower strength than IC-A.

3.3. Role of clinker fineness

Two types of blended cement formulations were prepared using (a) fine attrition milled clinker (X_{50} = 3.6 μm), and (b) coarse ball milled clinker (X_{50} = 55.2 μm). The formulation, AMC50S and BMC50S contained attrition milled slag (X_{50} = 5.7 μm). Fig. 3 shows the variation in compressive strength of cement with time for AMC50S and BMC50S. The strength at all times is comparable for AMC50S and BMC50S, indicating that clinker fineness is not critical.

3.4. Characterization of hydrated cement samples

3.4.1. X-ray diffraction studies

The analysis of XRD patterns (Fig. 4) of 1 and 28-day hydrated blended cements, AMC50 and IC-A, indicated presence of Quartz, Ettringite, Alite (C_3S), Belite (C_2S), Gehlenite (C_2AS) and portlandite (CH) phase. The variation in the characteristic peak of C_3S at ~0.304 nm and CH at 0.492 nm were examined in detail to monitor the progress of hydration. C_3S was consumed in the hydration reaction. The peak at 0.304 nm, which corresponds to strongest line of C_3S, decreased in IC-A due to its consumption during hydration from 1 to 28 days. However, a reverse trend was observed in the case of AMC50S. In order to find a possible explanation, the hydration of attrition milled slag was studied using XRD. Fig. 5 shows the XRD pattern of the unmilled granulated slag and attrition milled slag (5 and 10 min) after 28 days of hydration in water. The broad and diffuse background peak with maxima around $d \sim 0.30$ nm in the hydrated sample of non-activated slag is the result of the short-range order of the $CaO–SiO_2–Al_2O_3–MgO$ glass structure from unreacted slag [25]. Presence of C–S–H phases at 0.304 nm was similar to the one produced during the hydration of calcium silicate phases (C_3S and C_2S) [25,26]. In addition to the common C–S–H phases, the formation of α-C_2SH was observed in the hydration product of mechanically activated slag, characterised by the strongest d-spacing of

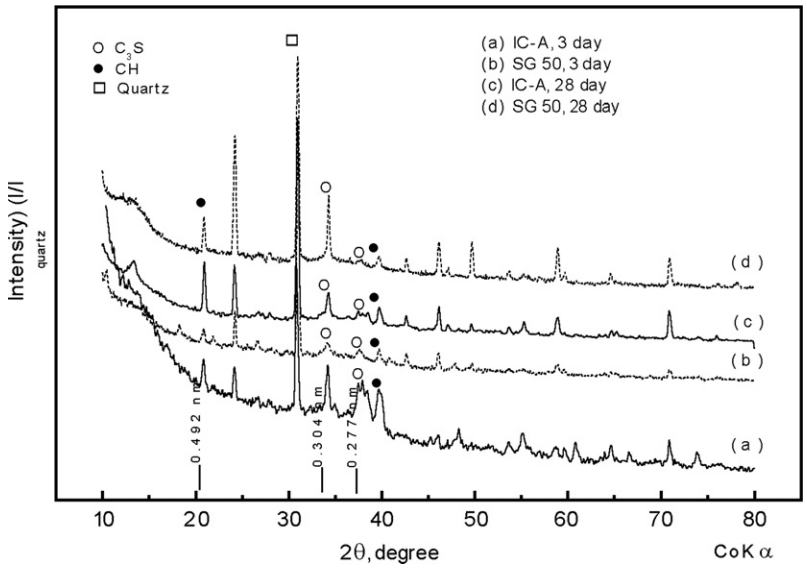

Fig. 4. XRD patterns of IC-A and AMC50S after hydration for 3 and 28 day.

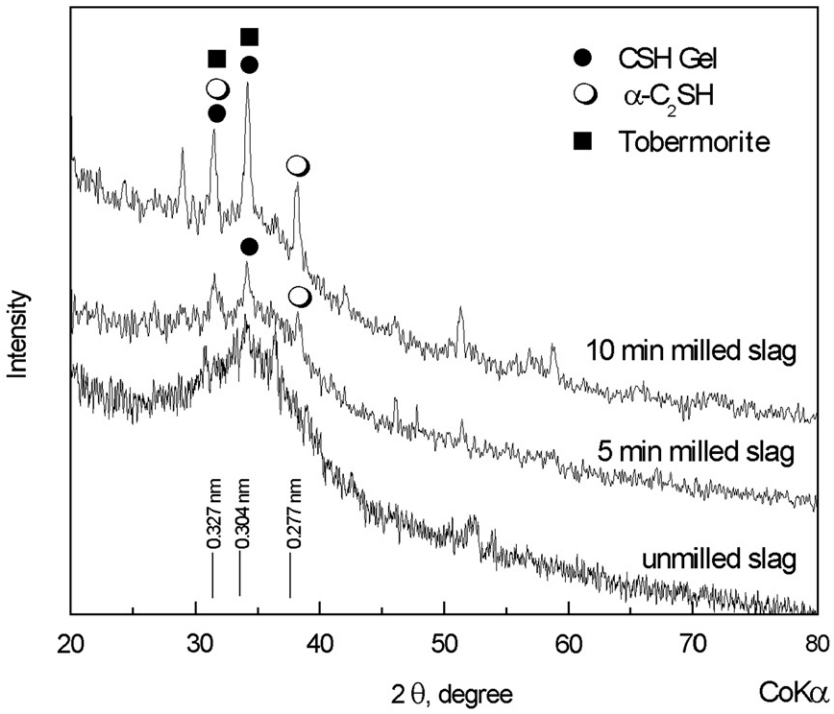

Fig. 5. XRD patterns of the unmilled granulated slag and attrition milled slag after 28 day hydration.

0.327 nm [27,28]. This means that the peak at 3.04 Å cannot be used alone to monitor the consumption of C_3S in the sample AMC50S. Alternatively, we used the 0.277 nm line of C_3S for monitoring the hydration. The relative intensity $[I/I_{quartz(max)}]$ of 0.277 nm line of C_3S followed the following order IC-A > AMC50S indicating that C_3S is consumed faster in the attrition milled samples than the commercial cement sample. This may be due to the finer slag particles which acted as nucleating agents for the formation of C–S–H and accelerated the hydration process. Unlike the unmilled slag, the mechanically activated slag was found to hydrate significantly depending upon the milling time. In sharp contrast to unmilled slag, the hydration product of milled slag was crystalline in nature and its crystallinity increased with an increase in milling time [20].

Hydration of C_3S and C_2S resulted in the formation of CH. CH formed during hydration reaction may be consumed in the hydration of slag. Thus, the intensity of characteristic peak of CH can be used as a measure of the reactivity of the slag; higher peak intensity signifying lesser consumption of CH and in turn, lesser reactivity of the slag. The CH peak intensity at 0.492 nm in AMC50S was lower than the IC-A after 1 and 28 days. This indicates the following: (a) the consumption of CH begins much earlier in the attrition milled samples than in the commercial sample; and (b) higher reactivity of slag in AMC50S due to mechanical activation resulting in greater consumption of CH. Higher reactivity of slag was also indicated by the background in XRD pattern that is attributed to the presence glass in the slag. It may be noted that the background was more pronounced in IC-A than AMC50S, especially after 1 day hydration, indicated greater amount of unreacted slag in IC-A.

3.4.2. Thermal analysis

Fig. 6a and b show the TG/DTA plots of AMC50S and IC-A sample, respectively, after 3 and 28 day hydration. Although the DTA plots of AMC50S and IC-A varied significantly from each other, generally, five distinct regions were observed for both the samples:

1. Region I up to 140 °C – this region was attributed to the dehydration of free water from hydrated cement matrix [29–32].
2. Region II from about 140–400 °C – this was the main temperature region of decomposition of cement hydration product (CSH, CAH, AFt and AFm phases) [29–32].
3. Region III from about 400–500 °C – this was the temperature region of decomposition of CH [29,30,32,33].
4. Region IV from about 500–750 °C – this region corresponds to decomposition of carbonate, hydrated aluminate and final stage of decomposition of C–S–H phases [29–33].
5. Region V above 750 °C – this was reported to be the region of recrystallisation of new phases arising from hydrated cement minerals [31–33].

In the DTA curve, the peak intensity in case of AMC50S was more pronounced at 441 and 574 °C in 3 day hydrated sample, which indicates that rate of early hydration. In IC-A, the peak intensity was almost similar in both 3 and 28 day hydrated samples. Weight loss corresponding to the decomposition of CH was determined from the TG plots. The weight loss was found to be 0.97% and 1.55% for the IC-A sample after 3 and 28 days of hydration. The weight loss for AMC50S was lower than IC-A, 0.88 and 0.91% after 3 and 28 days, indicating presence of lower amount of CH in the AMC50S. These results were consistent with the XRD results on CH in the AMC50S and IC-A.

3.4.3. Microstructural characterisation by SEM

Figs. 7 and 8 show typical SEM micrographs of hydrated cement samples. Largely, non-reacted slag particles, embedded in the hydrating clinker phase, were observed in IC-A after one day of hydration (Fig. 7a). Only after three days early signs of slag hydration were observed in IC-A. In contrast, formation of C-S-H gel in AMC50S was observed after one day indicating greater reactivity of slag due to mechanical activation. (Fig. 7b). Appearance of large portlandite crystals as thick as 20 μm could be observed in AMC50S after one day of hydration indicating significant hydration

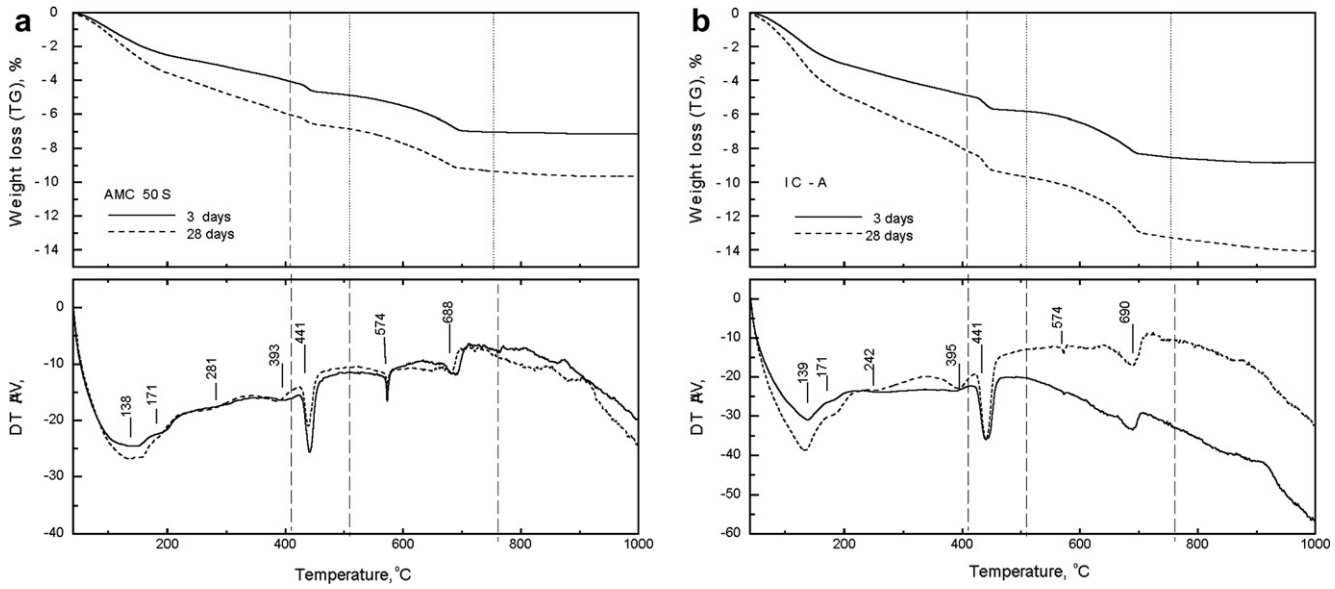

Fig. 6. TG/DTA plots of 3 and 28 day hydrated cement samples: (a) AMC50S, and (b) IC-A.

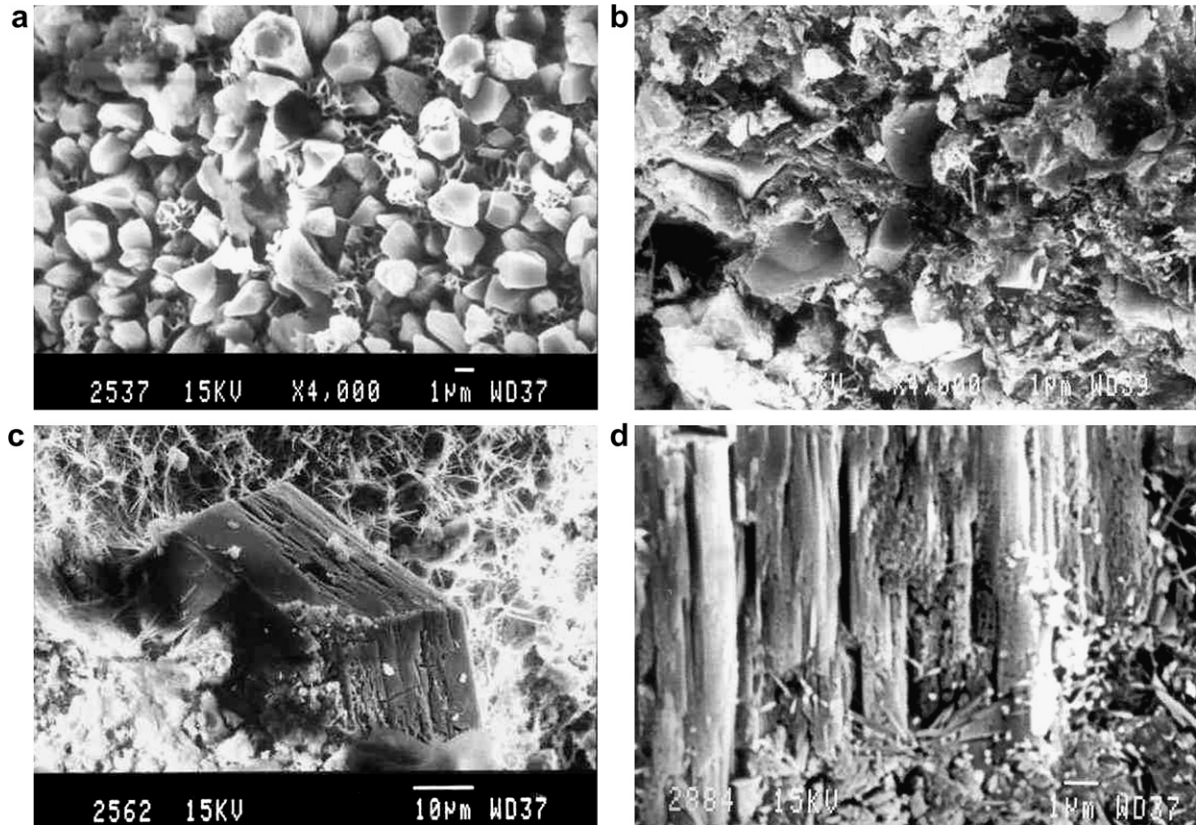

Fig. 7. SEM micrographs showing (a) mostly non-hydrated slag in IC-A after 1 day hydration, (b) hydrating slag in gel matrix in AMC50S after 1 day hydration, (c) large size portlandite crystal in AMC50S after 1 day hydration, and (d) columnar portlandite crystals in IC-A after 28 days hydration.

of calcium silicate phases and early formation of CH (Fig. 7c). Such big crystals of portlandite were not observed in IC-A. However, columnar crystals of portlandite are found after 28-days (Fig. 7d). The gel present in 28 days hydrated sample of IC-A had a honeycomb structure (Fig. 8a). The structure of gel phase formed in the sample containing mechanically activated slag was complex (Fig. 8b and c). Further, it was found that the structure of the sample containing mechanically activated slag becomes denser with increasing content of slag as shown for the AMC50S and AMC60S in Fig. 8b and c, respectively.

SEM-EDS studies revealed that in addition to Ca and Si as major elements, the hydration phases contained significant amounts of elements such as Mg and Al. Hence, we choose to calculate the [(Ca + Mg)/(Si + Al)] ratio along with the Ca/Si ratio. The typical

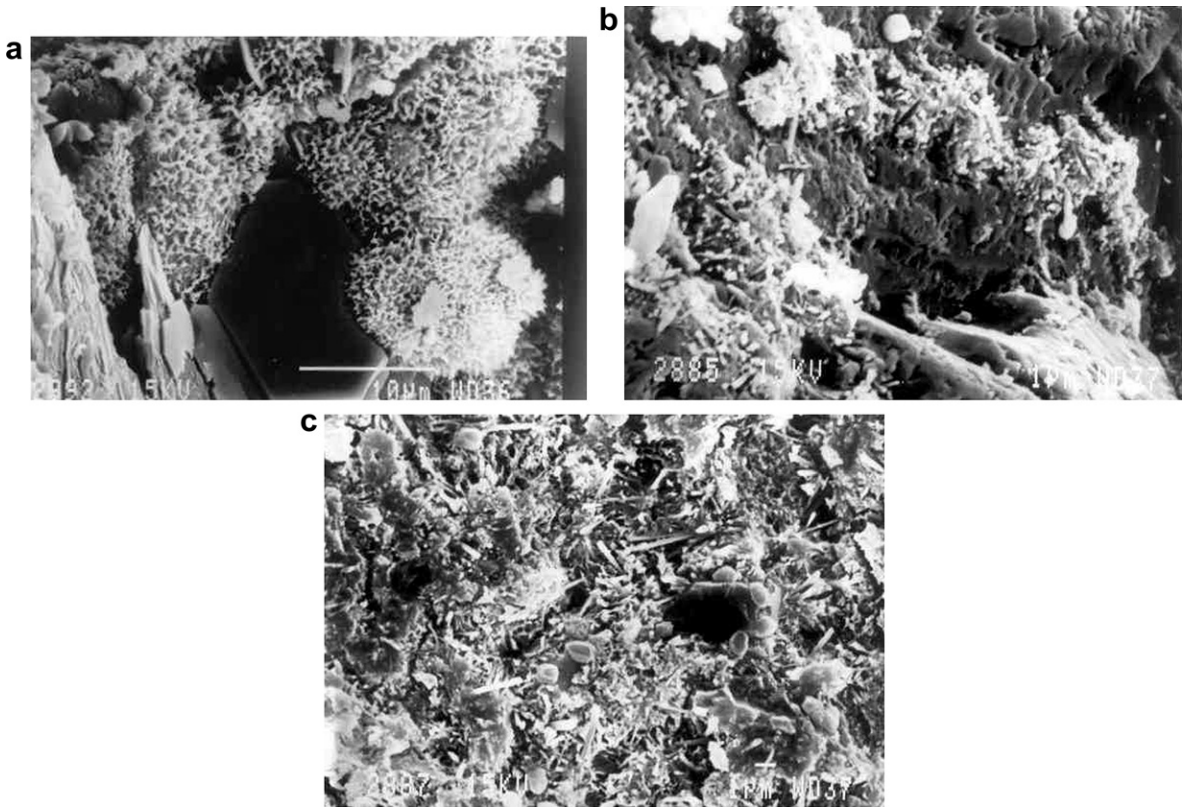

Fig. 8. Hydrated cement samples showing gel phase: (a) honeycomb structure of gel in IC-A after 28 day hydration, (b), (c) gel phase in AMC50S and AMC60S. AMC60S shows denser microstructure than AMC50S.

average molar Ca/Si ratios observed in IC-A after 48 h of hydration was 2.36, whereas the [(Ca + Mg)/(Si + Al)] ratios in case of AMC50S and AMC60S was 1.73 and 2.56, respectively. These ratios appear to be broadly in line with the phases identified by XRD.

3.4.4. Microstructure and properties

The strength development in all the tested cement samples, AMC50S and IC-A, is expected to depend on: (a) the hydration of clinker phases, (b) hydration of BF slag that has latent hydraulic activity and may also show pozzolanic character, (c) interaction(s) between the hydration of cement phases and slag. Overall the process of hydration and strength development is expected to be quite complex. Possible explanation for strength development is presented below in terms of reactivity of the constituents, evolution pattern of microstructure in different samples, porosity, etc.

XRD studies have indicated that tricalcium silicate phase in attrition milled samples (AMC50S) has higher reactivity than in commercial cement sample (IC-A). Based on the XRD and TG/DTA studies on hydrated cement samples, slag reactivity is also found to be higher in AMC50S than in IC-A. Thus, higher strength of cement containing the attrition milled slag may be correlated with the enhanced reactivity of slag particles. This is further supported by the strength attainment in cement containing very high volume of slag, which is developed due to enhanced hydraulic reactivity. Other factors which contributed in the strength development are the filler effect and pozzolanic effect of slag. The early consumption of CH gives an indirect indication of enhanced pozzolanic reactivity of slag. Important variables affecting solid reactivity include particles size (or surface area), state of aggregation, shape, defects etc. The X_{50} of AMC50S is 4.7 μm, is higher than IC-A that is characterised by a X_{50} value of 16.3 μm. Attrition milling is also found to result in angular particles with little or no aggregation. Thus, higher reactivity of attrition milled samples may be ascribed to a combined effect of lower particle size, angular shape and particles free from aggregation. The improved early strength development in AMC50S vis-à-vis IC-A may be related to the higher reactivity of cement phases and slag.

4. Summary and conclusions

This paper has presented results on the properties and microstructure of portland slag cement based on mechanically activated constituents, namely clinker and granulated blast furnace slag. The emphasis is on the activation of slag. An attrition mill is used for mechanical activation. The milling time for the slag is selected based on the particle size distribution and Zeta potential. The main conclusions of the study are

1. Mechanical activation of the slag has a beneficial effect on the early strength development. Low early strength development has been a major handicap in increasing the proportion of slag in conventional portland slag cement.
2. In the PSC prepared using mechanically activated clinker and slag, it was found that up to 85% replacement of clinker by slag is possible without impairing the strength vis-à-vis a commercial cement containing 40% slag of the same origin.
3. Unlike the ball milled slag, where strength decreases at early ages, both 1-day and 28-day strength increased with increasing amount of activated slag up to 70%
4. The fineness of the slag was found to be more critical than that of the clinker from the point of view of strength development.
5. Mechanical activation results in following changes in the evolution of microstructure during the hydration
   (a) increased hydration of C3S in clinker and hydration of slag due to the increase in its reactivity;

(b) early formation and consumption of CH; and
(c) more compact structure with increasing levels of the slag.

Acknowledgements

The authors would like to express their gratitude to Council of Scientific and Industrial Research (CSIR), New Delhi India for financial support under New Millennium Indian Technology Leadership Initiatives (NMITLI) programme. The slag and clinker samples used in the study were received from Grasim Cement, Rawan, Chattisgarh (India) and this is gratefully acknowledged.

References

[1] Chidiac SE, Panesar DK. Evolution of mechanical properties of concrete containing ground granulated blast furnace slag and effects on the scaling resistance test at 28 days. Cem Concr Comp 2008;30(2):63–71.
[2] Sharfuddin Ahmed M, Kayali O, Anderson W. Chloride penetration in binary and ternary blended cement concretes as measured by two different rapid methods. Cem Concr Comp 2008;30(7):576–82.
[3] Juhasz, Opoczky L. Mechanical activation of minerals by grinding: pulverizing and morphology of particles. NY: Ellis Horwood Limited; 1994.
[4] Dongxu Li, Xuequan Wu, Jinlin Shen, Yujiang Wang. The influence of compound admixtures on the properties of high-content slag cement. Cem Concr Res 2000;30(2000):45–50.
[5] Fu Xinghua, Hou Wenping, Yang Chunxia, Li Dongxu, Wu Xuequan. Studies on portland cement with large amount of slag. Cem Concr Res 2000;30:645–9.
[6] Boldyrew VV, Polov SV, Goldberg EL. Interrelation between fine grinding and mechanical activation. Int J Min Process 1996;44–45:181–5.
[7] Boldyrev VV. Mechanical activation of solid and its application to technology. J Chim Phys 1986;83(11/12):821–2.
[8] Venkateswaran D, Bhat IK, Cursetji RM. Mechano-chemical reactions induced by fine grinding of ordinary portland cement. In: Proceeding eighth NCB international seminar on cement and building materials, 18–21 Nov, New Delhi, India; 2003. p. 83–7.
[9] Kumar Sanjay, Bandopadhyay A, Rajinikanth V, Alex TC, Mishra IB, Singh KK, et al. Attrition milling for improved processing of blended cement. In: Proceeding eighth NCB international seminar on cement and building materials 18–21 Nov, New Delhi, India; 2003. p. 73–9.
[10] Kumar Sanjay, Bandopadhyay A, Rajinikanth V, Alex TC, Kumar Rakesh. Improved processing of blended slag cement through mechanical activation. J Mat Sci 2004;39:3449–52.
[11] Sobolev K. Effect of complex admixtures on cement properties and the development of a test procedure for the evaluation of high-strength cements. Adv Cem Res 2003;15(2):67–75.
[12] Sekulic Z, Popov S, Milosevic S. Comminution and mechanical activation of portland cement in different mill types. Ceram-Silikaty 1998;42(1):25–8.
[13] Kumar Sanjay, Rajinikanth V, Alex TC, Mittra BK, Khan ZH, Mishra IB, et al. Utilization of high volume of blast furnace slag and fly ash in blended cements through high energy milling. In: Lakshmanan N, Gopalakrishnan S, Sreenath HG, editors. Proc intl conf advances in concrete composites and structures. Chennai: Allied Publishers; 2005. p. 113–20.
[14] Kapur PC. Self-preserving size spectra of comminuted particles. Chem Eng Sci 1972;27:323–63.
[15] Kapur PC, Healy TW, Scales PJ, Boger DV, Wilson D. Role of dispersants in kinetics and energetics of stirred ball mill grinding. Int J Min Process 1996;47:141–52.
[16] Kolb G, Ott K. Efficient agitator bead mills. Euro Coal 1992;4:199–214.
[17] Bernhardt P. Investigations into process dynamics and control of a laboratory agitator bead mill. Int J Min Process 1996;44–45:629–34.
[18] Cho H, Waters MA, Hogg R. Investigation of the grind limit in stirred media milling. Int J Mineral Process 1996;44–45:607–15.
[19] Kwade A, Schwedes J. Breaking characteristics of different materials and their effect on stress intensity and stress number in stirred media mills. Powder Technol 2002;122:109–21.
[20] Kumar Rakesh, Kumar Sanjay, BadJena SK, Mehrotra SP. Hydration of mechanically activated granulated blast furnace slag. Met Mat Trans B 2005;36B:473–84.
[21] JCPDS X-ray powder diffraction file No. 35-0755 for gehlenite ($2CaO \cdot Al_2O_3SiO_2$).
[22] Taylor JC. Rietveld made easy: a practical guide to the understanding of the method and successful phase quantifications. Canberra: Sietronics Pty Ltd.; 2001.
[23] ACI Committee 233. Ground Granulated blast-furnace slag as a cementitious constituent in concrete. ACI Mater J 1995;92(3):321–2.
[24] Sobolev K. Mechano-chemical modification of cement with high volumes of blast furnace slag. Cem Concr Comp 2005;27:848–53.
[25] Song S, Jennings HM. Pore solution chemistry of alkali-activated ground granulated blast-furnace slag. Cem Concr Res 1999;29:159–70.
[26] Richardson IG. Tobermorite/jennite and tobermorite/calcium hydroxide-based models for the structure of C–S–H: applicability to hardened pastes of tricalcium silicate, β-dicalcium silicate, portland cement, and blends of portland cement with blast-furnace slag, metakaolin, or silica fume. Cem Concr Res 2004;34:1733–77.
[27] Chen JF, Thomas JJ, Taylor HFW, Jennings HM. Solubility and structure of calcium silicate hydrate. Cem Concr Res 2004;34:1499–519.
[28] Garbev K, Black L, Beuchle G, Stemmermann P. Inorganic polymers in cement based materials 1. Wasser Geotechnol Jahrgang 2002;Heft 2:19–30.
[29] Garbev K. Structure, properties and quantitative Rietveld analysis of calcium silicate hydrates (C–S–H Phases) crystallised under hydrothermal conditions. PhD Thesis, Institut fur Technische Chemie von der Fakultat fur Chemie und Geowissenschaften der Ruprecht-Karls-Universitat Hiedelberg, Germany; June 2004.
[30] Taylor HFW. Cement chemistry. 2nd ed. London: Thomas Telford Publication; 1998.
[31] Lea FM. The chemistry of cement and concrete. In: Hewlett PC, editor. 4th ed. London: Edward Arnold; 1998.
[32] Strydom CA, Potgieter JH. An investigation into the chemical nature of the reactivity of lime. In: Justness H, editor. Proceedings 10th international congress on chemistry of cement. Sweden: Gothenburg; 1997. p. 20–49.
[33] Mojumdar SC, Janokta I. Thermophysical properties of blends from Portland and sulphoaluminate-belite cements. Acta Phys Slovaca 2002;52(5):435–46.